ADVANCES IN COHERENT ELECTRON COOLING*

Vladimir N. Litvinenko for the CeC collaboration
Collider Accelerator Department, Brookhaven National Laboratory, Upton
Department of Physics, NY, USA

Abstract

Cooling techniques are required for improving the quality of hadron beams and increasing the luminosity in hadron- and electron-hadron-colliders. In contrast to light leptons that have very strong radiation damping via synchrotron radiation, the hadrons radiate very little (even in a 7-TeV LHC) and require an additional cooling mechanism to control the growth or reduce their emittances. In this paper, we focus on the advances in, and challenges of Coherent Electron Cooling (CeC) that promises to be an effective method of cooling of high-energy hadron beams, and potentially even ultra-relativistic muon beams.

Specifically, we describe the underlying physics principles, and the advances in this revolutionary, but yet untested, technique: viz., CeC. While we described physics principles in an earlier paper [1], our comprehensive studies revealed several other important factors affecting the CeC's performance [2-5]. In this paper, we summarize our main findings as well as presenting current advances and novel CeC schemes. We also briefly describe the CeC demonstration experiment under preparation at Brookhaven National Laboratory; its detailed description is part of these proceedings [6].

INTRODUCTION

In contrast to electron- and positron-beams, hadron beams in all present-day storage rings and colliders do not have strong loss mechanism, such as synchrotron radiation and, therefore, there is no natural mode of damping to reduce their energy spreads and emittances. Cooling hadron beams transversely and longitudinally at the energy of the collision may greatly increase the luminosity of high-energy hadron colliders and future electron-hadron colliders, such as the RHIC [7] eRHIC [8], ELIC [9], and even the LHC/LHeC [10]. The high luminosity of these colliders is critical for high-energy physics and in high-energy nuclear physics.

Presently, two techniques are used for efficiently cooling hadron beams; electron cooling [11], and stochastic cooling [12]. Unfortunately, the efficiency of traditional electron cooling rapidly falls with the increase in the beam's energy. Detailed studies of this technique for RHIC demonstrated that its efficiency declines as hadron energy to the power 2.5. Consequently, the cooling time for 250 GeV protons in RHIC would exceed 30 hours, a time that is too long, and the strength of this cooling is too feeble to affect luminosity in RHIC, eRHIC, or in ELIC. It also will not suffice for reducing the beam's emittance and the bunch length of hadron beams envisioned eRHIC.

The efficiency of traditional stochastic cooling, while independent of the particles' energy, rapidly falls with the particles' number and their longitudinal density [12].

Hence, while this technique has been very successful with ion beams, it is ineffective for proton beams with a typical linear density $\sim 10^{11}$-10^{12} protons per nanosecond. The eRHIC relies upon a very high longitudinal- and transverse-density of ions, with the growth times of intra-beam scattering (IBS) ranging from a few seconds to a few minutes. Present-day stochastic cooling [13] has cooling time $\sim$10-100 hours, and cannot offer the cooling required to attain high luminosity.

Accordingly, it is impossible to assure the cooling of protons with energies from about 100 GeV in RHIC (or eRHIC) with conventional techniques. However, two potential candidates might be up to the task; viz., optical stochastic cooling (OSC) [14], and coherent electron cooling (CeC) [1].

The OSC technique is very interesting but highly inflexible; it is based on a fixed wavelength laser amplifying undulator radiation from the hadron beam. Hence, it is hardly useable, if at all, for hadron colliders operating at various energies. For example, operating the RHIC at 50 GeV and 250 GeV with the same OSC system would necessitate changing the amplifier wavelength by a factor of 25, i.e., well beyond the capabilities of current lasers.

In contrast, the CeC technique is based on the fully adjustable optics-free FEL-amplifying mechanism [1]. Furthermore, it does not necessitate our making any changes in the system, neither to support a large range of the operational energies nor for cooling different species. In addition, the amplifier's wavelength naturally scales with the particles' energy.

Finally, there are CeC schemes that do not require the FEL as an amplifier, the so-called hybrid and bunching/micro-bunching schemes [15-19] that we discuss briefly in next session; however, they await a detailed evaluation of their performance.

COHERENT ELECTRON COOLING

The CeC scheme is based on the electrostatic interactions between electrons and hadrons that are amplified ether in a high-gain FEL or by other means. The CeC mechanism bears some similarities to stochastic cooling, but with the enormous bandwidth of the amplifier. Here, we briefly review the fundamental principles of physics involved in coherent electron cooling (CeC). Figure 1 is a schematic of a classical coherent electron-cooler, comprising a modulator, a FEL-amplifier, and a kicker. It also illustrates some aspects of the process of CeC.

Figures 2-4 depict three other schematics of the CeC using approaches other than an FEL amplifier [15-19]. These schemes are developed conceptually, and detailed studies still are essential, similar to that of the classical
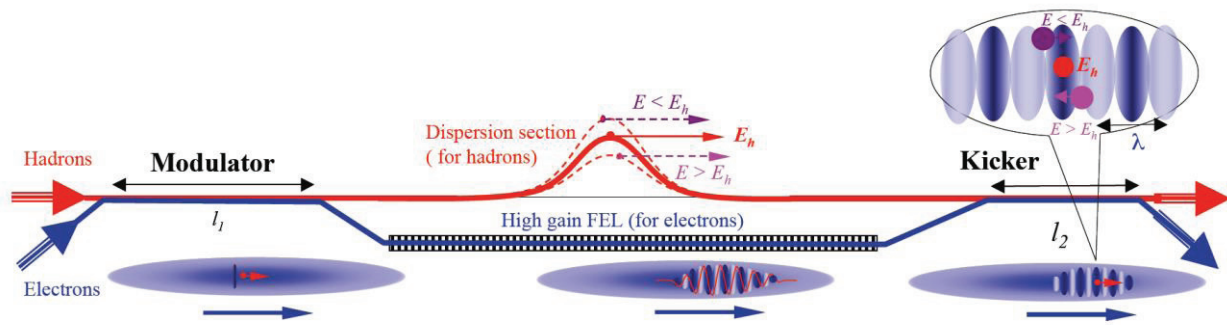
Figure 1: A general schematic of the classical Coherent Electron Cooler comprising three sections: A modulator, an FEL plus a dispersion section, and a kicker. For clarity, the size of the FEL wavelength, λ, is exaggerated grossly .
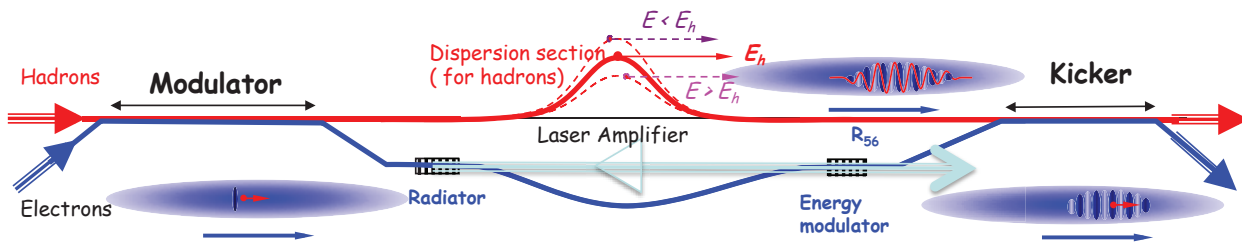

Figure 2: A hybrid CeC schematic uses a broad-band laser amplifying electron-beam's radiation from a short wiggler. The amplified laser power then, in a second wiggler, modulates the electrons energy. The latter is transferred into a density modulation using the R_{56} of an achromatic dog-leg.
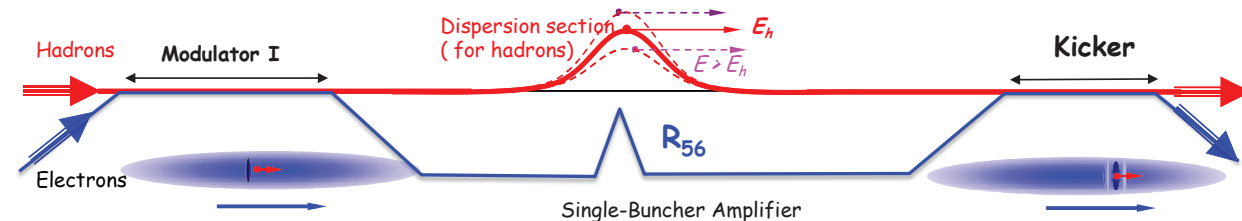

Figure 3: A CeC with an enhanced bunching by a single strong-field buncher. The scheme requires that the electron beam has special qualities [15-19].
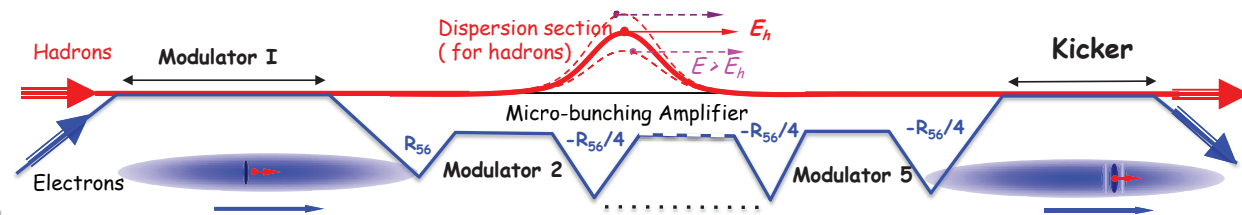

Figure 4: A layout of a CeC using a micro-bunching instability as an amplifier [17].

In contrast to the two schemes shown in Figs. 1 and 2, which have a limited bandwidth ~ 10^{14} Hz, the schemes shown in Figs. 3 and 4 essentially can generate a single wavelet of the bunch density and extend the CeC' bandwidth to ~ 10^{17} Hz.

CeC scheme, to support our evaluations of both their potential and their limitations. Hence, we first fully describe the physics of classical CeC and its drawbacks. Many of our conclusions are applicable to the other CeC schemes.

In the CeC, the electron- and hadron-beams have the same velocity, v:

$$\gamma_o = E_e/m_ec^2 = E_h/m_hc^2 = 1/\sqrt{1 - v^2/c^2} >> 1 \quad (1)$$

and co-propagate, in a vacuum, along a straight line in the modulator and the kicker; this is achieved by selecting the energy of electrons such that the relativistic factors γ of the two beams are identical.

The CeC works as follows: In the modulator, each hadron (with charge, Ze, and atomic number, A) induces density modulation in electron beam that is amplified in the high-gain FEL; in the kicker, the hadrons interact with the

beam's self-induced electric field and experience energy kicks toward their central energy. The process reduces the hadrons' energy spread, i.e., it cools the hadron beam.

In detail, within the modulator, each individual hadron attracts the surrounding electrons and generates an imprint of density modulation. In about a quarter of the plasma period, each hadron becomes surrounded by a cloud of electrons with a total charge equal to that of its own, but opposite in sign, i.e., it is shielded. In the co-moving frame, the longitudinal velocity-spread is much smaller than that in the transverse direction. Consequently, the transverse Debye radius greatly exceeds that in the longitudinal direction, and the electron cloud assumes a very flat, pancake-like shape.

These individual density-modulations are self-amplified when electron beam passes through a high-gain FEL into a wave-packet in the electrons' density.

This periodic density-modulation generates a periodic longitudinal electric-field. When the hadron recombines with the electron beam, it is exposed to this field. We select the delay between the self-induced wave-packet and a hadron such that a hadron with central energy (E_o) arrives at the kicker on the top of the electron-density peak, where electric field is zero. Hence, it does not experience any change in its energy.

The hadron's dispersion section imposes a time-of-flight dependence on the hadrons' energy . Thus, a hadron with higher energy than E_o reaches the kicker ahead of the negatively charged (high density) peak, and is dragged back (decelerated) by its self-induced electric field. Similarly, a hadron with lower energy than designed value enters the kicker behind the negatively charged (high density) peak and is pulled forward (accelerated) by the self-induced electric field. The outcome of this process is a reduction in the hadrons' energy spread, and the subsequent longitudinal cooling of the hadron beam.

In following sub-sections, we describe the main effects in each section of the CeC.

CeC Modulator

The co-moving frame (c.m.) of reference, where the electron- and hadron-beams are at rest, is the most natural one for describing the processes in the modulator. Therein, the motion of the electrons and hadrons is non-relativistic, and can be described from first principles. We note that the velocity spreads of the electrons and hadrons are highly anisotropic with $\sigma_{v_{x,y}} \gg \sigma_{v_z}$, where z is direction of beams' propagation. In the modulator, a positively charged hadron attracts electrons, creating a cloud of them around it. If the hadron moves with nearly-constant non-zero velocity, $\vec{v}_h = \hat{x}v_x + \hat{y}v_y + \hat{z} \cdot v$, the electron cloud follows it with some lag, $\Delta\zeta \propto v_z/\omega_p$. The typical dimensions of this disk-shaped electron cloud (a pancake) are given by the dynamic Debye radii:

$$R_{\Delta_\alpha} \mu \left(|v_\alpha| + \sigma_{v_\alpha}\right)/\omega_p; \quad \alpha = x, y, z,$$

where $\omega_p = \sqrt{4\pi n_e e^2/\gamma_o m_e}$ is the plasma frequency of electron beam in the c.m. frame, n_e is the lab-frame electron density, and, $-e$ and m_e, respectively, are the electron's charge and mass. We can show analytically (for an infinite plasma [20]) that a simple formula represents the total charge induced by the hadron in the electron plasma:

$$q = -Ze \cdot \left(1 - \cos\omega_p t\right), \qquad (2)$$

where Ze is the charge of the hadron. An exact solution was analytically derived [20] for the response on the presence of a hadron in a homogenous infinite electron beam with anisotropic κ-2 velocity distribution:

$$f(\vec{v}) = \frac{n_o}{\pi^2 \sigma_{vx}\sigma_{vy}\sigma_{vz}}\left(1 + \frac{v_x^2}{\sigma_{vx}^2} + \frac{v_y^2}{\sigma_{vy}^2} + \frac{v_z^2}{\sigma_{vz}^2}\right)^{-2}$$

with the solution of

$$\tilde{n}(\vec{r},t) = \frac{Zn_o\omega_p^3}{\pi^2\sigma_{vx}\sigma_{vy}\sigma_{vz}} \times$$

$$\int_0^{\omega_p t}\tau\sin\tau\left(\tau^2 + \sum_{\alpha=x,y,z}\left(\frac{\alpha - v_{h\alpha}\tau/\omega_p}{r_{D\alpha}}\right)^2\right)^{-2} d\tau$$

This result was used for testing simulations by Tech X Co. with VORPAL code [21] that currently can simulate modulators for an finite electron beam with arbitrary distributions [22].

The induced change can be in the order of that of the ion,

$$X = -\frac{q}{-Ze} \sim 1$$

for modest hadron-beam energies and a modest peak current of the electron beam. However, this is not applicable for the LHC with TeV-scale hadron beams when the phase-advance of the plasma oscillation is very small ($\omega_p t \ll 1$) and would result in negligibly small induced-charge:

$$X\mu\left(\omega_p t\right)^2/2 \ll 1$$

One solution to resolving this problem is using a compensated chicane as a buncher [16] after the modulator. In a modulator with the length L, the hadron will induce an energy modulation of the electrons beam depending on their relative longitudinal position to the hadron:

$$\left\langle\frac{\delta E}{E}\right\rangle \cong -2Z\frac{r_e}{a^2}\cdot\frac{L}{\gamma_o}\cdot\left(\frac{z}{|z|} - \frac{z}{\sqrt{a^2/\gamma_o^2 + z^2}}\right) \qquad (3)$$

where a is the radius of electron beam. An exact analytical solution of the Vlasov equation for this case is possible in an impulse model [18]. For a Gaussian energy-distribution RMS spread, σ_ε, in electrons the longitudinal density is given by following expression:

$$\tilde{\rho}(z \cdot R_{56}\sigma_\varepsilon) = \pi c_o \cdot \int_0^\infty Y\, dY \cdot \left\{\frac{Erf\left(\frac{Y - \Omega Y^{-2} + z}{\sqrt{2}}\right) + Erf\left(\frac{Y - \Omega Y^{-2} - z}{\sqrt{2}}\right)}{1 - \Omega Y^{-3}} - Erf\left(\frac{Y + z}{\sqrt{2}}\right) - Erf\left(\frac{Y - z}{\sqrt{2}}\right)\right\};$$

where $\Omega = Z \cdot r_e L / R_{56}^2 \gamma_o^3 \sigma_\varepsilon^3$, r_e is the classical electron's radius, and R_{56} is the longitudinal dispersion of the buncher [18]. A typical distribution of induced charge is shown in Fig. 5. For a wide beam, the peak of such distribution contains

$$N_e \approx 4\pi Z n_o \frac{r_e L |R_{56}|}{\gamma_o} \qquad (4)$$

of electrons, which is proportional to the buncher's longitudinal dispersion [18, 19], while its width is proportional to its product on the relative energy spread of electrons. Thus, the maximum induced-charge can be increased to the limits set by the space charge [23].
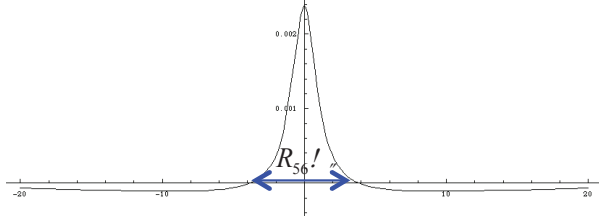

Figure 5: Profile of the induced density modulation in the modulator-buncher section.

Modulator-Buncher Based CeC

Hence, such bunching can be used to increase the induced charge in classical CeC, or to use this effect directly in enhanced bunching CeC, shown in Fig. 3.

Figure 4 shows the CeC scheme wherein this process is applied periodically to facilitate micro-bunch instability and to increase the induced bunch's density beyond that in Eq. (4) while keeping a similar spiked induced- density profile and the same duration [17]. The bandwidth of the CeC based on the bunching is determined by the duration of the density spike,

$$\Delta f \cong c / \left(R_{56} \sigma_\varepsilon \right)$$

and could be in the 10^{17} Hz range [17,18]. While looking very promising and potentially cost-effective, these schemes require detailed studies. One potential complication is the need for a very high R_{56} value that might significantly delay the electrons. To assure that the hadrons interact with the self-induced spike in the e-beam, the delay of the hadrons should be equal to that of electrons. Achieving the latter may require a very strong and large magnetic system to delay the hadron beam and also to match its longitudinal dispersion to the value required for optimum cooling (discussed in the kicker section).

CeC Amplifier

We start this discussion again from the classical CeC scheme with the FEL serving as amplifier of the microscopic modulation of the e-beam's density imprinted by hadrons in the modulator.

An FEL is a resonant instability at the wavelength of

$$\lambda_o = \lambda_w \left(1 + \langle \vec{a}_w^2 \rangle \right) / 2\gamma_o^2; \ k_o = 2\pi / \lambda_o,$$

where λ_w is the wiggler's period and $\vec{a}_w = e\vec{A}_w / mc^2$ is the its dimensionless vector potential . If the longitudinal extent of an induced perturbation is considerably shorter than the FEL wavelength, it will be amplified similar to the shot noise (δ-functions in z-direction), a case well known in the theory of SASE FELs [24]. Since we are interested in a linear regime of FEL amplification, a response on a δ-function-like density perturbation can be described by a Green function:

$$\delta n = G_\tau(z - z_o), \ G_\tau(z) = \mathrm{Re}\, G_o(z) e^{ik_o z}, \qquad (5)$$

that, in turn, is described by its envelope and phase

$$G_o(z) = |G_o(z)| e^{i\phi(z)}.$$

While analytically exploring the evolution of the density modulation wave-packet originating from a δ-function-like perturbation to the best possible extent, [25-27], we took full advantage of the well-tested 3D FEL code Genesis 1.3 [28] to detail its evolution [3, 29].

Figure 6 below shows a typical simulated Green function for a FEL operating in the visible range [3, 4].
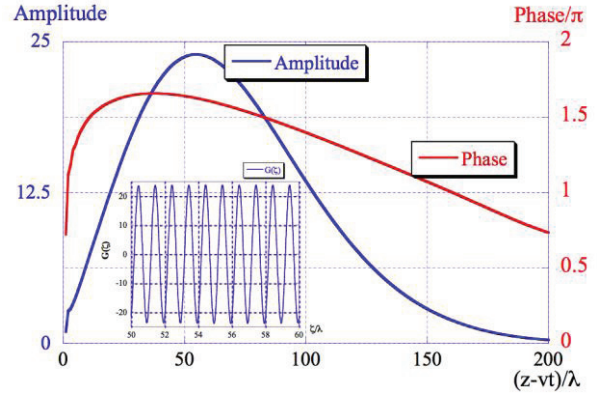

Figure 6: The amplitude (blue line) and the phase (red line in units of $\lambda_o/2$) of the FEL-gain envelope (Green function) after 7.5 amplitude gain-lengths (300 periods). The total slippage in the FEL is 300 λ_o, λ_o =0.7 μm. The clip shows the central part of the full gain function within the range of $\zeta = \{50\, \lambda_o, 60\, \lambda_o\}$ wavelets. The δ-like initial perturbation is located at ζ=0 wavelet.

We also explored the evolution of the wave packet as it propagates along the FEL [3, 4, 29]. In short, its evolution can be described as follows : During four gain-lengths, the peak density remains in its original state, propagating with the longitudinal velocity of the electron beam, e.g., slipping behind the light for one FEL wavelength per wiggler period. Its amplitude falls slightly because of the dephasing caused by energy spread and emittance. At the same time, a wave-packet of the optical wave, energy, and density modulation starts forming in front of the perturbation. After about 4 gain-lengths, the amplitude of the density modulation (bunching factor) in the wave-packet reaches the level of the initial perturbation; thereafter, growth is nearly exponentially, as depicted in Fig. 7.
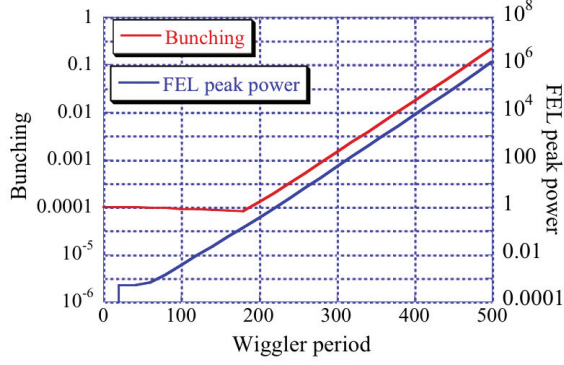
Figure 7: Evolution of the e-beam peak of the bunching factor and the FEL power simulated by the code Genesis. Gain length for the optical power is 1 m (20 periods) and for the amplitude/modulation, it is 2m (40 periods). [3, 4]

We also found [3,4] that group velocity of the wave-packet was slightly lower than the predicted 1D FEL theory value of $v_{gr1D} = (c + 2\langle v_{ze} \rangle)/3$, and is closer to

$$v_{gr3D} = (c + 3\langle v_{ze} \rangle)/4 \cdot$$

There also is an additional delay of the wave-packet occurring during the formation period, as detailed in [3,4].

Since the delay in the formation of the wave-packet is about 4 gain-lengths, the maximum gain of the density modulation (i.e., the maximum value of the Green-function) is less than a simple exponential estimate for the amplification in a continuous wave in an FEL, $G_{1DCW} \cong \exp[L_w / L_g]/3$, where L_g is the amplitude e-fold gain length of the FEL.

The gain limitation in FEL, as in other electron- beam instabilities, results from saturation. It can be treated in model-independent way for a case wherein the initial density perturbation comprise a random, uncorrelated shot-noise. Thus, the results are applicable to any amplifier of density perturbation in CeC schemes; details of the derivation appear in [30].

In a case of the CeC, the initial signal is the direct sum of

$$\delta n_o = \sum_{i, electrons} \delta(z - z_i) + X \sum_{j, hadrons} \delta(z - z_j)$$

where z_i and z_j correspondingly are the longitudinal locations of electrons and Debye ellipsoids, at the entrance of the amplifier. In the linear regime as in Eq.(5), the amplified density becomes

$$n_o(\tau, z) = n_o + \sum_{i=1}^{N_e} G_\tau(z - z_i) + X \sum_{j=1}^{N_i} G_\tau(z - z_j)$$

It is well known that e-beam instabilities, including that in FEL, are described by a set of self-consistent Maxwell and Vlasov equations. In its classical limit, Maxwell equations are completely linear. The latter is not true for the Vlasov equation; hence, it is responsible for the saturation, which occurs when the e-beam's density modulation be-

comes comparable with the initial beam's density: $|\delta n| \sim n_o$.

Using the randomness of the short noise in both the electron- and hadron- beams, we readily show [30] that Green function is limited by the following equation:

$$|g_{max}| \leq \sqrt{\frac{\hat{N}_e}{N_c\left(1 + X^2 \cdot \frac{\hat{N}_h}{\hat{N}_e}\right)}} \qquad (6)$$

with $g(z) = \int_{-z}^{\lambda_o - z} G_\tau(\zeta) e^{ik_o\zeta} d\zeta^*$ being the amplification of the bunching factor (i.e.., the parameter typically used in FEL theory and simulations), where $\hat{N}_e = \lambda_o I_e / ec$ and $\hat{N}_h = \lambda_o I_h / Zec$ are number of electrons and hadrons, correspondingly, per wavelength, and N_c is the Green-function correlation length in units of the wavelength:

$$N_c = \frac{\int |G(z)|^2 dz}{\lambda_0 |G(z)|^2_{max}} \propto \frac{\omega}{\delta\omega}$$

that is inverse proportional to the amplifier's relative bandwidth [30]. In practical units Eq. (5) becomes

$$g_{max} \leq 144 \cdot \sqrt{\frac{I_{pe}[A] \cdot \lambda_o [\mu m]}{N_c\left(1 + \frac{X^2}{Z} \cdot \frac{I_h}{I_e}\right)}}$$

where N_c can be estimated from the FEL formulae, or, which is much more accurate, can be calculated from a simulated Green function. For example, the Green function shown in Fig.6 has $N_c \cong 38$ corresponding to FEL amplification bandwidth of 1.13×10^{13} Hz.

Formula (6) was checked with direct simulations using Genesis 1.3 [29] for wavelength from tens of nm to tens of microns; it showed an excellent agreement within 10-20%.

Studies of saturation clearly demonstrated that the Grenn-function envelope stops growing at saturation (or even falls), and, after few gain-length passes, its phase has become randomized, e.g., cooling would stop working. It proved our assumption that we have to use only the linear response of the FEL. As a practical limit for Green-functions, we do not exceed 50% of the limit in Eq. (6).

It is important that Eq. (6) applies to the other CeC schemes shown in Fig. 3-4. The advantage of the bunching schemes is that $N_c \sim 1$.

CeC with Laser Amplifier

As indicated in Fig. 2 and Fig. 8, a broad-band laser amplifier can be used to amplify the density modulation in

*We note that for δ-function $|g|_{max} = 1$ as easily can be seen from $g(z) = \int_z^{\lambda_o + z} \delta(z - z_i) e^{ik_oz} dz = e^{ik_oz_i} \vee z_i \in \{z, z + \lambda_o\}$;

an electron beam. This initial modulation is imprinted in the radiation from a short wiggler (tuned to the laser's wavelength). Modern laser amplifiers, especially optical parametric amplifiers (OPA) operating in or near IR have a large bandwidth reaching towards few 10^{13} Hz, high gain and low noise [31, 32]. Hence, wigglers with few wiggler periods N_w should be used to keep the large bandwidth of the system of $N_c \sim N_{claser} + 2N_w$.
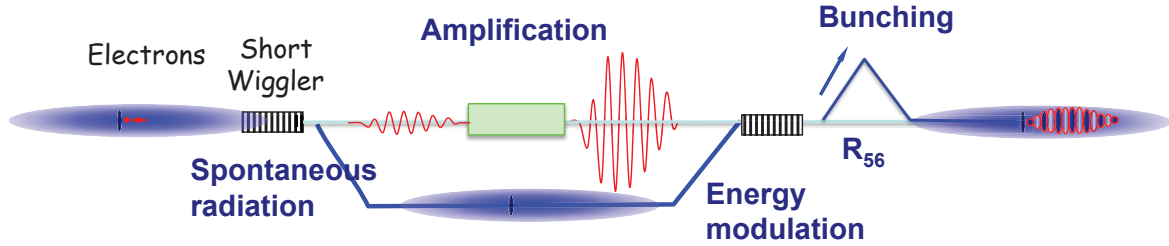

Figure 8: Details of the laser amplifier scheme for the CeC.

When it is amplified, it modulates the electron's energy in the second wiggler. The latter becomes translated into a density perturbation. Naturally, the limit in the gain in density modulation in 2 (6) also directly applies to this scheme.

While looking simpler and likely less expensive than an FEL amplifier, the laser-amplifier-based CeC would be required to accommodate a few-cm delay for a hadron beam, associated with light delays in the laser amplifier and the windows required to extract and inject light from and to the vacuum system. Such a delay system for 100-Gev- to TeV-scale hadron beams could be very complicated and very expensive. Hence, the advantages of this scheme should evaluated for a specific project.

CeC Kicker

CeC employs a longitudinal electric field self-induced by a hadron in form of density modulation in electron beam to correct the energy of the hadron. Since the value of the longitudinal electric field does not change when transferred from co-moving to the laboratory frame, it is easiest task to calculate the field in a co-moving (cm) frame, where electron beam is at rest. In the latter case, the transverse sizes of the beam are that same as in the laboratory frame, while the longitudinal size is boosted by the Lorentz factor: in the cm frame, the density is modulated with period of

$$\lambda_{ocm} = \gamma_o \lambda_o; \; k_{ocm} = k_o / \gamma_o,$$

When the transverse size of the beam is significantly larger that the modulation period $\sigma_\perp >> \gamma_o \lambda_o$, the electric field is practically one-dimensional and can be easily calculated from its density modulation:

$$\mathbf{E}_z = -4Xe \frac{|g|}{A} \sin(k_o z / \gamma_o + \phi); \quad (7')$$

where $A = 2\pi\beta_\perp \varepsilon_{n\perp} / \gamma_o$ is the transverse area of electron beam expressed through its β-function and normalized emittance. For a transverse beam whose size is comparable with the modulation wavelength in cm frame

$$\rho(\vec{r}) = \rho_o(r) \cdot \cos(kz);$$

we can use analytical field expressed through modified Bessel functions [33]:

$$\varphi(\vec{r}) = -4\pi \cos(kz) \left\{ I_0(kr) \int_r^\infty \xi K_0(k\xi) \rho_o(\xi) d\xi + K_0(kr) \int_0^r \xi I_0(k\xi) \rho_o(\xi) d\xi \right\}$$

with longitudinal field on axis given by

$$E_z = -4\pi k \sin(kz) \int_0^\infty \xi K_0(k\xi) \rho_o(\xi) d\xi.$$

Figure 9 below shows how the fields on the axis depend of the product of the the size of the transverse beam and the modulation wave-number. For practical purposes, we use $k_o \sigma_\perp / \gamma_o$ from 1.5 to 5, where a reduction either is insignificant or not dramatic.
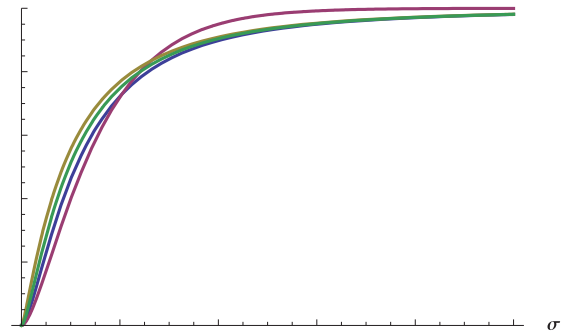

Figure 9: Normalized dependence of the electric field on the e-beam's axis as function of $k_o \sigma_\perp / \gamma_o$. When $k_o \sigma_\perp / \gamma_o >> 1$, the field value approaches that of the 1D limit in Eq. (7).

For an infinite plasma, the evolution of the density modulation in the kicker can be studied analytically [34] (the equations are the same as for the modulator [20], but the initial conditions differ). However, the VOPRAL code is perfectly suited for simulating both the dynamics of, and for calculating the electric fields induced by the modulation [22].

Our studies shows that density modulation continues growing after leaving the FEL and propagating in the modulator. This continues for about a quarter of plasma oscillation. They also confirmed that Eq. (7) is a reasonable estimate with an accuracy factor ~2 (frequently underestimating the field). Naturally, for a real system, we use

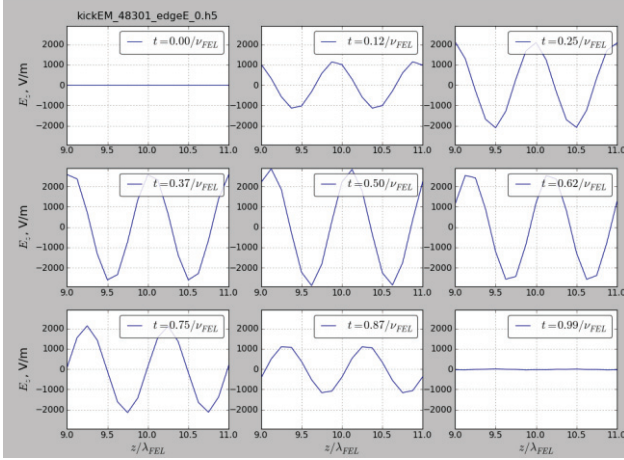the results of simulations, a sample of which are shown in Fig. 10.

Figure 10: Evolution of longitudinal electric field in the kicker, simulated by VORPAL [21, 22]; the first clip at t=0 intentionally is left empty.

Since the longitudinal electric field induced in electron beam is frame independent, Eq. (7) rewrites as:

$$\mathbf{E}_z = -E_o \sin\left(k_o(z - \mathrm{v}t) + \phi\right); \qquad (7')$$

and use it for estimating the energy kick experienced by a hadron. As we discussed in the introduction, the delay and the longitudinal dispersion, D, of the hadron transport line is important for the cooling process. First, the delay should be adjusted such that the hadron arrives to the kicker at the same time as the arrival of the crest of the wave-packet envelope (induced by the hadron); this assures an optimum electric field. A microscopic path-length adjustment applied to electron beam (less than one FEL wavelength, called a phase adjustment in optical klystron) could be used to ensure that the hadron with center (design) energy, $\mathbf{E_o}$, arrives at the crest of the electron density, where longitudinal electric field is zero. Thus, hadrons with ideal energy do not experience any energy change. A hadron with an energy deviation would experience an electric field and its energy would change as follows:

$$\frac{d\mathbf{E}}{dz} \cong -eZE_o \cdot \sin\left(k_o \cdot D \frac{\mathbf{E} - \mathbf{E}_o}{\mathbf{E}_o}\right).$$

Assuming that the size of the electron beam matches that of the hadron beam and that the length of the kicker is equal to the hadron's beta-function $l \sim \beta_\perp$, we can estimate the energy kick as

$$\Delta \mathbf{E} \sim -ZXe^2\gamma_o \frac{2|g|}{2\pi\varepsilon_{n\perp}} \sin\left(k_o \cdot D \frac{\mathbf{E} - \mathbf{E}_o}{\mathbf{E}_o}\right); \qquad (8)$$

with $\chi = k_o \cdot D\sigma_\varepsilon \sim 1$ being the natural choice for the dispersions.

Cooling

Equation (8) is the source of the longitudinal cooling: Within $|k_o \cdot D(\mathbf{E} - \mathbf{E}_o)/\mathbf{E}_o| < \pi$, hadrons with high energy are decelerated, and hadrons with low energy are accelerated. Consequently, all the beam within this margin

is cooled. Averaging over hadron's synchrotron oscillations $(\mathrm{E}-\mathrm{E}_o)/\mathrm{E}_o = a \cdot \cos\left(\omega_s n + \phi_s\right)$ yields

$$\left\langle \frac{a'}{\sigma_{\delta h}} \right\rangle = -\zeta \cdot J_1\left(\chi \frac{a}{\sigma_{\delta h}}\right); \zeta \approx \frac{2|g_{max}|}{\pi\varepsilon_{n\perp}} \frac{ZXr_p}{A};$$

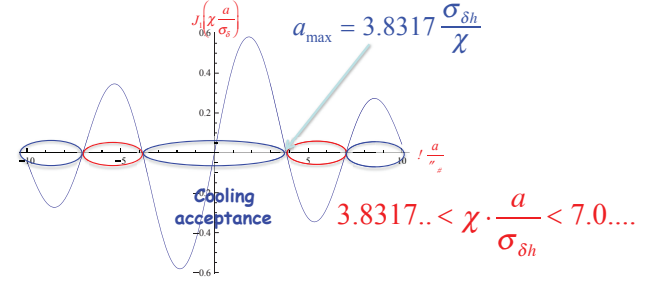with the damping and anti-damping ranges shown in Fig. 11.

Figure 11: Damping (blue) and anti-damping zones (red) for the synchrotron oscillations of hadrons.

We note that the bunching/micro-bunching version of CeC would not have any anti-cooling energy-zones . The charge induced in such scheme (Fig. 5 or [17]) generates a longitudinal non-oscillating electric field (i.e., it crosses zero only at z=0) and would dampen all energy deviations. It is one of important advantages of this scheme

As we described earlier [1,16], in a classical CeC scheme, transverse cooling could be assured via coupling of transverse and longitudinal degrees of freedom. Similar to the redistribution of the decrements of synchrotron-radiation damping, we can redistribute the longitudinal damping of the CeC process to transverse directions:

$$\xi_l + \xi_{t1} + \xi_{t2} = \xi_{CeC}.$$

where t1 and t2 represent two transverse modes of betatron motion (for uncoupled motion, it is simply x and y).

The easiest way to couple to the transverse motion (for example, x) is to install a chromatic chicane for the electron beam after the FEL, so to tilt the slices of density modulation (Fig. 8) and to make the electric field also dependent on x:

$$\Delta E_{h,i} = \Delta E_o\left(k\left(D_l\delta + R^e_{26}x\right)\right)$$

In combination with non-zero transverse dispersion ($\eta_x \neq 0$) in the location of the kicker, this scheme couples the longitudinal- and transverse-cooling

$$\xi_\perp = \xi_{CeC o} \frac{\eta_x}{D_l} R^e_{26}$$

Proper coupling between the horizontal- and vertical-motions, which is controllable with skew-quadrupoles or by operating close to a coupling resonance, further redistributes $\xi_\perp$ between the two betatron modes.

For example, in the CeC for 250 GeV protons in RHIC/eRHIC, using an electron chicane with $R^e_{26}=10^{-3}$ and hadron's horizontal dispersion of 5 cm in the kicker would split the cooling equally between three degrees of freedom. The optimal split between the cooling decrements should be determined by the corresponding IBS rates and other sources of diffusion; calculating them is beyond scope of this paper.

The bandwidth of the CeC also can limit the maximum cooling rate. As was shown in [1], the rate of CeC cooling rate could not exceed that rate set by the limit on stochastic cooling:

$$\xi_{CeC\,\max} = \frac{2}{N_{eff}}\left(kD\sigma_\varepsilon\right) \qquad (9)$$

where,

$$N_h \frac{\Lambda_k}{\sqrt{4\pi}\sigma_{z,h}} + \frac{N_e}{X^2}\frac{\Lambda_k}{\sqrt{4\pi}\sigma_{z,e}}; \Lambda_k = N_c\lambda_o$$

is effective number of hadrons interacting in CeC process, e.g. the so-called the number of particles in the sample.

The latter limit may become important either for a very high density of the hadron beam (e.g., in eRHIC, we plan to have $\sim 10^{12}$/nsec particle density in proton beam) or when a very short cooling times in large accelerators (e.g., the LHC) are required.

For a given charge of an electron bunch, our study showed that optimal cooling rates can be obtained by long electron bunches whose length is comparable to that of the hadron bunch. Reducing the length of electron bunch would require so-called painting, reducing average cooling as the ratio of the bunch lengths of the hadron and electron bunches.

In turn, this would require a faster instantaneous rate of cooling, which could exceed the limit set by Eq. (9).

Examples of the CeC

In Table 1, we summarize most important parameters and our estimates for three test case for CeC: A proof-of-principle CeC experiment with a 40-GeV Au ion beam, 250 GeV eRHIC's and 7 TeV LHC's proton beams.

Table 1: CeC Estimates

Parameter	CeC PoP	eRHIC	LHC
Species	Au	p	p
Energy, GeV	40	250	7000
Particles per bunch	10^9	2×10^{11}	1.7×10^{11}
ε_n, mm mrad	2	0.2	3
Energy spread	$3.7\ 10^{-4}$	10^{-4}	10^{-4}
RMS bunch length, nsec	3.5	0.27	1
e-beam energy MeV	21.8	136.2	3812
Peak current, A	75	50	30
ε_n, mm mrad	5	1	1
RMS bunch length, nsec	0.05	0.27	1
Modulator, m	3	10	100, plus a buncher
Kicker, m	3	10	100

Parameter	CeC PoP	eRHIC	LHC
FEL length, m	7.5	9	100
λ_w, cm	4	3	10
λ_o, nm	13,755	422	91
a_w	0.5	1	10
g_{max}	650	44	17
g (used)	100	3	8.5
CeC bandwidth, Hz	$6.2\ 10^{11}$	$1.1\ 10^{13}$	$2.4\ 10^{13}$
Cooling time, hours, estimate	0.1	0.12	0.4
-//- local, sec	4		

PROOF-OF-PRINCIPLE EXPERIMENT

Since CeC is novel technique that never has been tested, we have, since 2011, been pursuing an experimental demonstration of this technique using linear acceleration and a RHIC ion- beam at 40 GeV/u. Our goal is to simulate the CeC performance and thereafter demonstrate it experimentally by cooling a single bunch of ions. The project is supported the DoE's Office of Nuclear Physics and Brookhaven Science Associates.

We plan to start the commissioning of this system in 2015. Details of this experiment are described elsewhere in these proceedings [6].

REFERENCES

[1] V.N. Litvinenko, Y.S. Derbenev, Physical Review Letters 102, 114801 (2009)

[2] G. Wang, V. Litvinenko, S.D. Webb, "Amplification of Current Density Modulation in a FEL with an Infinite Electron beam", Proceedings of 2011 Particle Accelerator Conference, New York, NY, USA, March 25-April 1, 2011, pp. http://jacow.org/PAC2011 /papers/thp149.pdf

[3] Y. Hao, V. Litvinenko, "Simulation Study of Electron Response Amplification in Coherent Electron Cooling", Proceedings of Third International Particle Accelerator Conference, New Orleans, USA, May 20 - 25, 2012, p. 448, http://jacow.org/IPAC2012/papers/moppd038.pdf

[4] V.N. Litvinenko et al., Progress with FEL-based coherent electron cooling", Proceeding of 30th International Free Electron Conference, Gyeungju, Korea, August 24-29, 2008, p.529, http://jacow.org/FEL2008/papers/thdau05.pdf

[5] G. Wang, M. Blaskiewicz, V.N. Litvinenko, "Progress on Analytical Modeling of Coherent Electron Cooling", Proceedings of First International Particle Accelerator Conference, IPAC'10, Kyoto, Japan, May 23-28, 2010, p.873, http://jacow.org/IPAC10/papers/mopd077.pdf

[6] I. Pinayev et al., "Recent Status of Coherent Electron Cooling Proof-of-Principle Experiment", WEPP014, COOL 2013, Mürren, Switzerland

[7] V.N.Litvinenko, Potential for polarized luminosity increases at RHIC with CeC, BNL, July 31, 2009

[8] V.N.Litvinenko et al., Proceedings PAC 2005

[9] A. Bogacz et al., Proceedings of PAC 2005

[10] LHC design report, http://documents.cern.ch/cgi-bin/

[11] S.Nagaitsev et al., Phys. Rev. Lett. 96, 044801 (2006)

[12] S. van der Meer, Rev. Mod. Phys. 57, 689 (1985)

[13] M.Blaskiewicz, J.M. Brennan, F Severino, Physical Review Letters 100, 174802 (2008)

[14] A.Mikhalichenko, M.Zolotorev, Phys. Rev. Lett., 71, p.4146 (1993)

[15] V.N. Litvinenko Coherent Electron Cooling, C-AD seminar, BNL, May 2008

[16] V.N. Litvinenko, Y.S. Derbenev, Proc. of 29th International Free Electron Laser Conference, Novosibirsk, Russia, 2007, p. 268, http://jacow.org/f07/PAPERS/TUCAU01.PDF

[17] D.F. Ratner, "Microbunched electron cooling for hadrons", SLAC-PUB-15346, SLAC, Menlo Park, California, April 3, 2013, submitted to Physics Review Letters

[18] V.N. Litvinenko, CeC Modulator with a Buncher, C-AD internal note, April 22, 2008

[19] V.N. Litvinenko, G. Wang, D. Ratner, Enhanced bunching, unpublished.

[20] G.Wang, M.Blaskiewicz, Phys Rev E, volume 78, 026413 (2008)

[21] G.I. Bell et al., "VORPAL Simulations Relevant to Coherent Electron Cooling", European Particle Accelerator Conference 2008 (EPAC'10), Genoa, Italy, 2008, p. 3185 http://jacow.org/e08/papers/thpc085.pdf

[22] B. Schwartz et al., "Coherent Electron Cooling: Status of Single-Pass Simulations," Proceedings of the 4th International Particle Accelerator Conference (IPAC 2013), MOPWO071 (2013).

[23] V.N. Litvinenko, Space charge limit for a buncher, C-AD note

[24] E.L. Saldin, E.A. Schneidermiller, M.V. Yurkov, The Physics of FELs, Springer, 1999

[25] G. Wang, V.N. Litvinenko, S.D. Webb, 32th International Free Electron Laser Conference, Malmo, Sweden, 2010, p. 60. http://jacow.org/FEL2010/papers/mopb04.pdf

[26] G. Wang, M.Blaskiewicz, V.N. Litvinenko, Particle Accelerator Conference 2009 (PAC09), Vancouver, British Columbia, Canada, 2009, p. 1460. http://jacow.org/PAC2009/papers/tu6pfp074.pdf

[27] S.D. Webb, V. N.Litvinenko, G. Wang, 32th International Free Electron Laser Conference, Malmo, Sweden, 2010, pp. 52. http://jacow.org/FEL2010/papers/mopb02.pdf

[28] S. Reiche, Genesis 1.3, http://genesis.web.psi.ch/aboutgenesis.html

[29] Y. Jing et al., Simulation studies of FEL Green function and its saturation, to be published in Proc. of 2013 FEL conference, August 2013, New York, USA

[30] V.N. Litvinenko, On limit of FEL gain, C-A/AP/480, technote, BNL, March 2013, http://public.bnl.gov/docs/cad/Documents/On%20the%20FEL%20Gain%20Limit.pdf

[31] J. Moses, et al., Opt. Lett. 34, 1639-1641 (2009)

[32] K.-H. Hong, et al, Opt. Lett. 33, 2473 (2008)

[33] G. Wang, V.N. Litvinenko, Electric field of a modulated beam, C-AD internal note

[34] G. Wang et al., Proceedings of IPAC'10, Kyoto, Japan, 2010, p.873, http://epaper.kek.jp/IPAC10/papers/mopd077.pdf